

RESEARCH ARTICLE

Resource-Constrained Multi-objective Optimization Model for Global Warming Resilient Emergency Response and Welfare Networks

* OMINIGBO O. J., OMETAN S. O., EBAIFIYEGHA A. E., KAYOH C. O. AND OKEDOYE M. A.

Department of Mathematics, Federal University of Petroleum Resources, Effurun, Nigeria..

Corresponding Email: ojayominigbo@gmail.com

Received: 10-07-2025; Revised: 15-08-2025; Accepted: 11-09-2025

ABSTRACT

This study introduces an uncertain multi-objective, multi-commodity, multi-period, and multi-vehicle mixed-integer programming model with social equity designed for the critical response phase of humanitarian operations. The framework strategically addresses the complexities of disaster relief by integrating five key echelons: affected regions, distribution centers, hospitals, temporary accommodation facilities, and temporary care centers. The model is driven by four primary objectives: the minimization of overall costs associated with facility location, resource allocation, social equity and crucially, the reduction of relief supply shortages. Uncertainty inherent in disaster scenarios is robustly managed through a probabilistic scenario-based approach. Significant strategic decisions facilitated by the model encompass the optimal siting of temporary care and accommodation centers, the efficient allocation of affected populations to designated centers and hospitals, and the effective distribution of supplies from major hubs to temporary shelters. Furthermore, the model determines optimal flows for injured individuals and commodities between facilities, specifies the required number of vehicles for inter-facility transport, and manages both shortage and inventory levels at all centers. A comprehensive set of constraints ensures practical applicability, covering aspects such as demand fulfillment, relief commodity flow, facility capacities, transportation logistics for both people and goods, and the utilization of backup centers across multiple planning periods.

The developed model's efficacy was demonstrated through its application to a real-world case study: the city of Warri and its environs in Nigeria, a region significantly impacted by floods exacerbated by global warming. To solve this complex problem, three distinct methods were employed: the epsilon-constraint method, the Non-Dominated Sorting Genetic Algorithm-II (NSGA-II), and a modified multi-objective particle swarm optimization (MMOPSO). Performance analysis, utilizing various multi-objective evaluation metrics, confirmed the superior performance of MMOPSO. A significant innovation of this model is its inherent integration of social equity principles, ensuring that the allocation of resources and services prioritizes the most vulnerable populations within the affected area. A preferred solution, selected from the MMOPSO-generated non-dominated set based on these equity considerations and expert judgment, was thoroughly analyzed to exemplify the model's practical implications for resilient and equitable disaster response.

Keywords: : Humanitarian Logistics, Multi-objective Optimization, Uncertainty, Flood Disaster, Social Equity, Location- Allocation, Global warming

INTRODUCTION

The accelerating impacts of global warming have significantly heightened the frequency, intensity, and complexity of natural disasters, including floods, droughts, heatwaves, and hurricanes. These events pose a critical threat to public welfare, particularly in vulnerable and resource-scarce regions. As climate change continues to disrupt environmental stability, the ability of emergency response systems to adapt and respond efficiently is increasingly constrained by limited resources, uncertain demand, damaged infrastructure, and competing socio-economic priorities. The increasing impact of global warming on the frequency, magnitude, and unpredictability of disasters has been well-documented. According to the IPCC Sixth Assessment Report (2023), global mean surface temperatures are projected to rise by 1.5 C to 2 C within the next few decades, amplifying the risk of floods, droughts, wildfires, and hurricanes. Consequently, emergency response systems are experiencing heightened stress, especially in low- and middle-income countries. Traditional disaster response models primarily focus on logistics optimization, often assuming availability of sufficient resources for effective implementation. For example, Rawls and Turnquist (2016) proposed stochastic optimization approaches to pre-position emergency supplies, improving delivery speed while accounting for uncertainty in demand. However, these models typically optimize single objectives, often neglecting distributional fairness or equity outcomes, especially for socially vulnerable populations (Kellermann et al., 2018). Rahmani and Ghasemi (2022) developed an integrated multi-objective location-inventory-routing problem (LIRP) tailored for humanitarian relief supply chains under the increasing threat of global warming-induced disasters. The model simultaneously addresses decisions regarding the location of distribution centers, inventory pre-positioning, and vehicle routing for post-disaster relief delivery. Uniquely, it incorporates the impacts of global warming, such as increased disaster frequency and severity, into both demand uncertainty and transportation network vulnerability to balances cost, responsiveness, and fairness in aid distribution and successfully improves logistical preparedness and responsiveness in humanitarian supply chains facing the growing risks posed by climate change. Results demonstrate that considering climate-induced uncertainties in pre-positioning strategies leads to more resilient and equitable relief operations. Trade-off analysis enables decision-makers to balance costs, delivery time, and equity according to specific disaster contexts and policy priorities. Emerging research emphasizes the integration of climate adaptation planning into emergency logistics, yet operational models that explicitly include climate-driven risk factors remain limited (Djalante et al., 2020). This highlights a crucial gap: the need for optimization models that simultaneously handle operational efficiency, social vulnerability, and climate-induced uncertainty. Designing resilient emergency response and welfare networks under these conditions necessitates advanced decision-support systems that can handle multiple, often conflicting objectives, such as minimizing response time, reducing operational costs, maximizing coverage, and ensuring equity among affected populations. These systems must also be capable of operating under uncertainty, incorporating environmental, logistical, and social risk factors into planning and execution. To address these challenges, mathematical optimization models have emerged as powerful tools in disaster management, enabling decision-makers to allocate scarce resources strategically and equitably. The formulation of a Resource-Constrained Multi-objective Optimization Model (RC-MOM) for climate-resilient emergency response requires interdisciplinary insights from three major research domains: climate-induced disaster response systems, optimization under resource constraints, and welfare network design. This section synthesizes relevant literature to situate the proposed work in relation to existing research.

Resource-constrained optimization is central to operations research and disaster logistics. Classical models include the capacitated vehicle routing problem (CVRP), knapsack problem, and facility location problems under budget or supply limitations (Farahani et al., 2009).

Several works have explored multi-commodity flow models where multiple types of relief supplies are transported across disrupted networks (Zheng et al., 2019). Multi-objective optimization models, in particular, offer a flexible framework for balancing the competing goals inherent in emergency and welfare logistics. However, most existing models either neglect resource constraints or fail to integrate fairness and climate resilience systematically. This paper proposes a novel resource-constrained multi-objective optimization model that explicitly incorporates equity, uncertainty, and climate resilience into the design of emergency response and welfare networks. The proposed model aims to bridge the methodological gap between operational efficiency and social justice in humanitarian logistics under global warming conditions.

LITERATURE REVIEW

The use of optimization techniques in disaster and humanitarian logistics has evolved significantly over the past two decades. Early models primarily focused on cost minimization and shortest-path routing without adequately accounting for resource limitations or social equity (Tzeng et al., 2007; Barbarosoglu and Arda, 2004). However, with the increasing complexity of disasters exacerbated by climate change, recent research has shifted towards more sophisticated multi-objective and resource-aware models. Mathematical optimization has played a pivotal role in shaping disaster response strategies, particularly through models that guide resource allocation, facility location, and logistics planning. Traditional approaches often prioritized cost minimization and logistical efficiency (Tzeng et al., 2007), but growing recognition of climate risks and social inequities has shifted attention toward more complex, multi-objective frameworks. Ahmadi et al. (2015) developed a humanitarian logistics model that considers network failures and resource constraints. Their approach integrates uncertainty using scenario-based stochastic programming, but equity was not explicitly addressed. Similarly, Rawls and Turnquist (2010) proposed a two-stage stochastic programming model for emergency resource allocation that emphasizes risk minimization. While effective under uncertain demand, their model did not incorporate fairness measures or climate-related disruptions. Recent studies have emphasized the need for climate-resilient humanitarian networks. For instance, Ransikarbun and Mason (2016) introduced a goal programming model balancing cost, response time, and fairness. Their work marks a notable effort in including equity considerations, though it does not fully address dynamic climate-related variables. Likewise, Mohammadi et al. (2022) proposed a robust optimization framework for resource allocation under uncertainty, accounting for social vulnerability and supply chain resilience. However, their model primarily operates within static conditions and lacks adaptability to evolving climate risks. Yazdani et al. (2021) proposed a dynamic network reconfiguration model in climate-induced flood scenarios. Their work reflects an emerging trend of integrating environmental modeling into logistics optimization. However, their focus was primarily on network topology and did not explore social or equity implications. Wang et al. (2021) explored the use of renewable energy-powered UAVs in emergency logistics. Their work highlights sustainable logistics innovations and suggests adaptability under resource constraints, though integration into equity-driven multi-objective models remains limited. Torabi et al. (2018) designed a resilient supply chain model using a bi-objective robust optimization approach that accounted for cost and service level. The model considers facility disruption and supply uncertainty but lacks attention to social vulnerability or fairness in outcomes. A growing body of literature also incorporates UAVs (Unmanned Aerial Vehicles) and renewable energy logistics in disaster response models to enhance flexibility and reduce environmental impact (Torabi et al., 2018; Wang et al., 2021). These innovations suggest that resilience and sustainability must be integrated into optimization models for global warming contexts. However, few existing models synthesize these dimensions into a unified, multi-objective framework under strict resource constraints. Moreover, the concept of equity and fairness in optimization has gained traction, with metrics such as the Gini coefficient and max-min fairness being employed to reduce disparity in resource allocation (Yuan et al., 2023). Yet, incorporating such metrics into climate-adaptive emergency logistics remains underdeveloped. Ghasemi and Khalilzadeh (2019) applied chance-constrained programming to humanitarian

logistics, capturing the probabilistic nature of demand and resource availability. Their model addresses stochasticity but does not include long-term resilience or social objectives.

Liu et al. (2023) employed a hybrid solution technique that combines evolutionary search with fairness metrics. However, it requires extensive calibration and lacks real-time adaptability. Zhu et al. (2020) used a max-min fairness model to allocate emergency shelters, ensuring that the worst-off individuals received priority. This aligns with social justice goals but may not be optimal from a cost perspective. Akbari and Salman (2017), addresses emergency resource allocation by formulating two multi-objective robust optimization framework incorporating uncertainty in demand using scenario-based approaches. The model focuses on simultaneously minimizing operational costs and the risks associated with the shortage of critical resources. It emphasizes balancing efficiency and robustness to ensure that emergency responses remain effective despite unpredictable disaster conditions without integrating dynamic uncertainty and real-time updates to refine allocation strategies. They used ϵ -constraint and weighted sum methods to generate Pareto-optimal solutions, evaluated on simulated disaster scenarios. Wu and Cui (2021), developed a bi-objective mixed-integer programming (MIP) model integrating flood hazard scenarios derived from climate change projections for evacuation planning in flood-prone regions, explicitly incorporating the increasing risks posed by global warming by minimizing both total evacuation time and inequality in evacuation routes among affected populations of the flood-prone urban areas using simulated global warming-augmented scenarios. By considering the intensified flood risks associated with climate change, the study emphasizes the need for adaptive evacuation strategies that ensure both efficiency and fairness without Incorporate real-time flood forecasting data and behavioral factors such as evacuation hesitancy. Li et al. (2022), introduces an equity-oriented optimization model for post-disaster resource allocation, explicitly addressing the role of social vulnerability in humanitarian logistics by incorporating social vulnerability data into optimization models for more equitable allocation outcomes, albeit with marginal increases in overall costs. The model integrates social vulnerability indices into resource allocation decisions to promote fairness alongside operational efficiency. Tofighi et al. (2016) proposed a multi-objective optimization model for designing humanitarian logistics networks under conditions of resource scarcity and the need for equitable distribution of aid by incorporates fairness considerations explicitly into the facility location and allocation decisions in the aftermath of disasters. The aim is to improve social equity by minimizing the disparity in aid delivery while considering cost-effectiveness. Uncertainty in demand is also addressed through robust optimization techniques, providing solutions that are resilient under varying disaster scenarios. This research fails to incorporate dynamic and time-dependent aspects of disaster relief logistics, including evolving demand patterns and multi-period decision frameworks. Additionally, integrating behavioral aspects of equity perception among affected populations and decision-makers could further enhance the applicability of such models in real-world humanitarian operations. Chen et al. (2022), proposed a model that effectively reduces inequality in resource distribution among disaster shelters without significantly increasing overall operational costs. By explicitly integrating equity into the optimization framework and ensures more balanced and socially just disaster response outcomes without considering multi-period and dynamic resource flows, reflecting the evolving nature of disaster impacts. Additionally, integrating community participation mechanisms and feedback loops in the allocation process can enhance legitimacy and acceptance of the resource distribution plans. Investigating the interplay between equity and other objectives like environmental impact. Jabbarzadeh et al. (2016), formulated a multi-objective optimization model for designing resilient and sustainable humanitarian supply chains, explicitly considering resource limitations. The model addresses challenges in disaster relief operations, such as budget constraints, transport capacity, and storage capacity to reflect real operational limitations in disaster response. Limited funding, constrained logistics capacities, and the necessity for environmentally sustainable operations. It integrates resilience strategies (e.g., multiple sourcing, redundant facilities) with sustainability considerations to improve operational performance. The trade-offs between economic efficiency, environmental impact, and operational resilience are systematically explored without focusing on dynamic models that adapt to real-time disaster developments, incorporate multi-period planning, and integrate behavioral factors such as stakeholder risk preferences. The inclusion of

social sustainability objectives, such as equity in beneficiary service levels or community engagement, is also recommended to complement environmental and resilience goals. Daneshvar and Khadem (2022), develops a robust multi-period optimization model for designing humanitarian relief supply networks under the uncertainties associated with global warming. Recognizing that climate change leads to increased variability in disaster frequency, severity, and logistics disruptions, the model addresses the need for resilient supply chains that can operate effectively over multiple planning periods. The model simultaneously considers uncertainties in demand fluctuations, transportation disruptions, and resource availability, offering a holistic approach to climate-resilient disaster logistics and substantially improves supply chain resilience in the face of climate-induced uncertainties. By planning for worst-case scenarios, the model guarantees continuity of relief operations even under severe disruptions. Although ensuring robustness slightly increases operational costs, the security and stability it offers make it highly suitable for humanitarian agencies operating in global warming-affected regions. Moradi and Manzouri (2024), proposes a resilient optimization model for designing food distribution networks during climate-induced crises. Recognizing that global warming exacerbates risks such as floods, droughts, and storms, the model seeks to ensure continuous, equitable, and efficient food supply during disruptions. The study integrates concepts of resilience and fairness in supply chains to provide actionable guidance for policymakers and humanitarian organizations working to maintain food security during complex emergencies. The findings show that while building resilience in food distribution incurs additional upfront costs, it significantly reduces the risk of severe supply shortages during major climate disruptions. Moreover, incorporating equity objectives prevents disproportionate suffering among marginalized communities. The integrated approach helps balance operational efficiency, social fairness, and long-term system sustainability. Mohammed et al. (2019), proposes an evolutionary algorithm-based framework for optimizing emergency resource allocation in disaster response scenarios. Given the uncertainty and time-critical nature of disasters, traditional optimization techniques often fall short in generating feasible solutions within tight deadlines. The authors introduce an evolutionary computation-based approach to rapidly search for near-optimal resource allocation strategies while addressing multiple, conflicting objectives such as cost minimization, equity, and response effectiveness. Their results show that evolutionary algorithms can generate high-quality, near-optimal solutions in shorter computational times compared to exact methods. Particularly under high uncertainty and tight deadlines, evolutionary approaches provided robust and adaptable resource allocation plans. While classical methods yield optimal solutions, their computational expense often renders them impractical in real-time disaster situations without integrating evolutionary optimization techniques into decision-support systems for disaster relief agencies. Further work should explore hybrid metaheuristic algorithms combining evolutionary algorithms with local search heuristics to improve convergence speed and solution quality.

MATHEMATICAL MODEL

The research introduces a multi-objective, multi-commodity, multi-period, multi-vehicle mixed-integer programming model designed to address challenges related to global warming impacts. The main assumptions underpinning this model are outlined below:

The model is developed for a planning horizon encompassing multiple time periods, specifically focusing on the aftermath of events exacerbated by global warming.

Five echelons are incorporated into the model: impacted regions, distribution hubs, healthcare facilities, temporary shelters, and emergency care centers.

The Four primary objective functions considered are the cost of humanitarian logistics operations and the extent of relief supply shortages. Crucially, these objectives are pursued with social equity as a guiding principle, ensuring that aid distribution prioritizes fairness and addresses the needs of vulnerable populations.

Model uncertainties, including the probability of extreme weather events (intensified by global warming), the likelihood of temporary shelter failure, and the probability of emergency care center failure, are addressed using a probabilistic scenario-based approach.

Multiple scenarios, each with an associated probability of occurrence, are developed based on the severity of global warming-induced events.

This model is applied to make strategic evacuation and relief efforts in the post-disaster phase following global warming-related incidents.

The number and locations of healthcare facilities and impacted regions are predetermined.

The capacities of all facilities are known.

The distances between impacted regions, distribution hubs, healthcare facilities, temporary shelters, and emergency care centers are known.

The load-carrying capacity of each vehicle type is known.

Provisions for backup temporary shelters and emergency care centers are included.

Multiple temporary shelters are considered, categorized as either vulnerable or resilient to global warming impacts.

Multiple emergency care centers are considered, categorized as either vulnerable or resilient to global warming impacts.

Several healthcare facilities with known capacities are available throughout the planning periods.

Multiple distribution hubs can be established to provide commodities.

All distances between facilities are fixed and known for the duration of the planning periods.

Demand for resources varies based on each specific scenario.

The indices, parameters, and decision variables employed in the model are presented as follows:

Sets and Indices

Sets:

F_D : Collection of temporary care facilities vulnerable to damage from global warming impacts, $F_D = \{1, \dots, F_D\}$

F_R : Collection of temporary care facilities resilient to global warming impacts, $F_R = \{1, \dots, F_R\}$

A_D : Collection of temporary accommodation centers vulnerable to damage from global warming impacts, $A_D = \{1, \dots, A_D\}$

A_R : Collection of temporary accommodation centers resistant to global warming impacts, $A_R = \{1, \dots, A_R\}$

Indices:

k : Index for potential sites of temporary accommodation centers, $k \in \{1, \dots, K\}$, where $K = A_D \cup A_R$

l : Index for potential sites of temporary care facilities, $l \in \{1, \dots, L\}$, where $L = F_D \cup F_R$

d : Index for regions impacted by global warming events, $d \in \{1, \dots, D\}$

h : Index for healthcare institutions, $h \in \{1, \dots, H\}$

e: Index for distribution hubs, $e \in \{1, \dots, E\}$

v: Index for transportation units, $v \in \{1, \dots, V\}$

c: Index for essential commodities (provisions), $c \in \{1, \dots, C\}$

s: Index for distinct global warming impact scenarios, $s \in \{1, \dots, S\}$

t: Index for sequential time periods, $t \in \{1, \dots, T\}$

r: Index for resource allocation tiers (0 for primary facilities, 1 to R for backup facilities), $r \in \{0, 1, \dots, R\}$

Parameters of the Model

Costs:

C^{care} : Cost associated with establishing a temporary care facility at location l at allocation tier r under scenario s .

C^{accom} : Cost associated with establishing a temporary accommodation center at location k at allocation tier r under scenario s .

C^{veh} : Operational cost per unit distance for vehicle v under scenario s .

Π^{care} : Penalty incurred for casualties at temporary care facility l during its failure due to global warming impacts in scenario s .

Π^{accom} : Penalty incurred for casualties at temporary accommodation center k during its failure due to global warming impacts in scenario s .

Demands:

$D^{\text{outpatient}}$: Number of individuals requiring outpatient services in affected region d under scenario s .

D^{evac} : Number of individuals needing evacuation from affected region d under scenario s .

D^{critical} : Number of critically injured individuals requiring treatment in affected region d under scenario s .

$Q^{\text{commodity}}$: Demand for commodity c at temporary accommodation center k during time period t under scenario s .

Capacities:

M^{patient} : Capacity of vehicle type v for transporting injured individuals (both critically and non-critically injured).

M^{evacuee} : Capacity of vehicle type v for transporting individuals displaced by global warming events.

M^{goods} : Capacity of vehicle type v for transporting various commodities.

N^{dist} : Capacity of distribution hub e for commodity type c under scenario s at time t .

N^{shelter} : Capacity of temporary accommodation center k for commodity type c under scenario s at time t .

N^{hospital} : Patient admission capacity of temporary care facility l across all allocation tiers r in scenario s .

N^{evacuee} : Capacity of temporary accommodation center k for evacuees under scenario s at allocation tier r .

Distances:

$D^{\text{affected-care}}$: Distance between affected region d and temporary care facility l at allocation tier r .

$D^{\text{affected-accom}}$: Distance between affected region d and temporary accommodation center k at allocation tier r .

$D^{\text{dist-accom}}$: Distance between distribution hub e and temporary accommodation center k at allocation tier r .

$D^{\text{affected-hospital}}$: Distance between affected region d and hospital h .

R^{care} : Coverage radius for temporary care facility l at allocation tier r .

R^{accom} : Coverage radius for temporary accommodation center k at allocation tier r .

Other Parameters:

$\Xi^{\text{equity}}_{dlsr}$: A disparity penalty coefficient for assigning affected area d to care facility l at allocation tier r in scenario s .

$\Xi^{\text{equity}}_{dksr}$: Disparity penalty for assigning affected area d to accommodation center k at allocation tier r in scenarios.

$P^{\text{care fail}}$: Probability of failure for temporary care facility $l \in F_D$ due to global warming impacts.

$P^{\text{accom fail}}_k$: Probability of failure for temporary accommodation center $k \in A_D$ due to global warming impacts.

M : A sufficiently large positive constant.

P_s : Probability of occurrence for scenario s .

β_{ct} : Consumption coefficient for commodity c in time period t .

γ_k : Minimum required coverage level for commodities at temporary accommodation center k .

ϑ_c : Volume (in m³) of each unit of commodity c .

ψ_c : Priority level for fulfilling the demand of commodity c .

Ω_{ds} is the vulnerability index of affected area d in scenario s .

Decision Variables

Location:

χ_{lsr} : 1, if a temporary care facility is established at location l at allocation tier r in scenario s

0, otherwise

k_{sr} : 1, if a temporary accommodation center is established at location k at allocation tier r in scenario s

0, otherwise

Allocation:

Z_{dlsr} : 1, if affected region d is assigned to temporary care facility l at allocation tier r in scenario s

0, otherwise

D_{ksr} : 1, if affected region d is assigned to temporary accommodation center k at allocation tier r in scenario s

0, otherwise

Flow Between Facilities:

Λ_{dls} : Number of non-critically injured individuals transferred from affected region d to temporary care facility l in scenario s .

D_{ks} : Number of individuals displaced by global warming impacts transferred from affected region d to temporary accommodation center k in scenario s .

D_{dhs} : Number of critically injured individuals transferred from affected region d to hospital h in scenario s .

Γ_{ekctst} : Quantity of commodity type c transferred at time t from distribution hub e to temporary accommodation center k in scenario s .

Number of Vehicles:

Y_{vdlst} : Number of vehicle type v traveling from affected region d to temporary care facility l in scenario s .

V_{dks} : Number of vehicle type v traveling from affected region d to temporary accommodation center k in scenario s .

Y''_{vdhs} : Number of vehicle type v traveling from affected region d to hospital h in scenario s .

Y_{vekst} : Number of vehicle type v traveling at time t from distribution hub e to temporary accommodation center k in scenario s .

Other Variables:

ω_{kctsr} : Amount of shortage for commodity c at temporary accommodation center k at allocation tier r in scenario s during period t .

τ_{kctst} : Amount of commodity c stored at temporary accommodation center k in period t in scenario s .

Building upon the established notation, the comprehensive mathematical model, defined by equations (1) — (29), is now presented. The objective function aims to minimize the total cost of humanitarian logistics and facility operations in the context of global warming impacts, by considering the sum of several cost components, along with minimizing the total shortage of critical supplies. It's composed of several parts, such that:

$$G_1 = \sum_{s=1}^S \sum_{d=1}^D D_{dhs} P_s \pi_{care} \sum_{l \in F_{dhs}} P_l^{care_fail} \zeta_{dlsr} + \sum_{k \in A_{dhs}} \sum_{r=0}^R (1 - P_k^{care_fail}) \zeta_{dksr} \quad (1)$$

Cost for casualties at temporary care facilities due to global warming impacts

$$G_2 = \sum_{s=1}^S \sum_{d=1}^D D_{dsk} P_s \pi_{accom} \sum_{k \in A_{dsk}} P_k^{accom_fail} \zeta_{dksr} + \sum_{k \in A_{dsk}} \sum_{r=0}^R (1 - P_k^{accom_fail}) \zeta_{dksr} \quad (2)$$

Cost for casualties at temporary accommodation centers due to global warming impacts

$$G_3 = \sum_{s=1}^S \sum_{v=1}^V \sum_{d=1}^D \sum_{l \in F_{dhs}} D_{dhl} Y_{vdlst} + \sum_{d=1}^D \sum_{r=0}^R \sum_{k \in A_{dhs}} D_{dks} Y_{vdkst} + \sum_{d=1}^D \sum_{h=1}^H D_{dhs} Y''_{vdhs} + \sum_{e=1}^E \sum_{r=0}^R \sum_{k \in A_{dhs}} \sum_{t=1}^T D_{ekctst} Y_{vekst} \quad (3)$$

Total transportation costs for vehicles across all routes and scenarios

$$G_4 = \sum_{s=1}^S P_s \sum_{r=0}^R \sum_{l \in F_{dhs}} C_{care} X_{lscr} + \sum_{r=0}^R \sum_{k \in A_{dhs}} C_{accom} X'_{kscr} + \sum_{k=1}^K \sum_{c=1}^C \sum_{t=1}^T \sum_{s=1}^S \sum_{r=0}^R P_s \psi_c \omega_{kctsr} + \sum_{s=1}^S \sum_{d=1}^D \sum_{l \in F_{dhs}} \text{equity}_{dlsr} + \sum_{k \in A_{dhs}} \text{equity}_{dksr} \quad (4)$$

Costs associated with establishing temporary care and accommodation facilities. Total weighted shortage cost of commodities. Penalty for inequitable aid distribution

To bolster the realism of the model, within the critical context of global warming impacts, we

introduce a component that explicitly accounts for social equity. This addition discourages solutions that inadvertently leave vulnerable populations underserved, reflecting a more holistic and ethical approach to humanitarian logistics. We define a penalty term, Ξ_{equity} , which quantifies the cost incurred when vulnerable groups in affected area d are inadequately served by temporary care facility l at allocation tier r in scenario s . This penalty should be a function of the vulnerability index of the affected area, Ω_{ds} , and could also consider factors like the distance to the facility or its capacity to serve the specific needs of vulnerable individuals. A mathematical expression for this equity-based penalty is:

$$\Xi_{equity}^{disc} = C^{eq} \times \Omega_{ds} \times \left[\frac{d_{l,c}^{affected-care}}{R_{care}^{w}} + \frac{1}{\sum_{r=0} N_{l,rs}^{hospital}} \right]$$

Here, C^{eq} represents a predefined societal cost or penalty multiplier associated with inequitable service provision. This value would need to be determined based on ethical and policy considerations. Ω_{ds} is the vulnerability index of affected area d in scenario s . A higher value indicates greater vulnerability, leading to a larger penalty if service is inadequate. This index could integrate various socio-economic, demographic, and health factors. $d_{l,c}^{affected-care}$ is the distance between affected area d and temporary care facility l in scenario s . A greater distance could imply increased difficulty in access for vulnerable groups. R_{care}^{w} is the maximum coverage distance for temporary care facility l at allocation tier r .

across all allocation tiers r in scenario s . Including the inverse of capacity ensures a higher penalty if a facility with limited capacity is disproportionately assigned vulnerable populations. Similarly, the concept of Ξ_{equity} is directly applicable to temporary accommodation centers as well. We can define a similar penalty term, Ξ_{equity} , to ensure

equitable service for vulnerable groups at temporary accommodation centers. Its mathematical expression would follow an analogous structure:

$$\Xi_{dksr} = C_{dksr} \times \Omega_{ds} \times \left[\frac{D_{dksr}^{\text{affected-accom}}}{R_{kr}^{\text{accom}}} + \frac{1}{N_{ksc}^{\text{evacuee}}} \right]$$

Here, $D_{dksr}^{\text{affected-accom}}$ is the distance to temporary accommodation center k , R_{kr}^{accom} is its coverage distance, and

$\sum_{r=0} N_{ksc}^{\text{evacuee}}$ represents its capacity for housing evacuees. By including both Ξ_{dlsr} and Ξ_{dksr} in the objective function, the model is encouraged to develop solutions that are not only cost-effective but also socially responsible, prioritizing the needs of the most vulnerable populations in global warming-induced disasters. Now, consolidating the various function to form the complete minimization problem, we say;

$$\min G1 + G2 + G3 + G4 \tag{5}$$

Subject to

$$\Lambda_{dhs} \leq \sum_{v=1} Y_{vdhs} M_v^{\text{patient}} \quad \forall d, l, s \tag{11}$$

$$\Lambda'_{dks} \leq \sum_{v=1} Y'_{vdks} M_v^{\text{evacuee}} \quad \forall d, k, s \tag{12}$$

$$\Lambda''_{dhs} \leq \sum_{v=1} Y''_{vdhs} M_v^{\text{patient}} \quad \forall d, h, s \tag{13}$$

$$\sum_{c=1} \Gamma_{ekcts} \leq \sum_{v=1} Y_{vekst} M_v^{\text{goods}} \quad \forall v, e, k, t, s \tag{14}$$

$$\sum_{d=1}^D \gamma_{dlk} \frac{\Omega_{dls}^{\text{affected-care}}}{R_{lk}^{\text{care}}} \leq \rho_{lk}^{\text{care}} \quad \forall l, r, s \tag{15}$$

$$\sum_{d=1}^D \sum_{ksc} \Lambda'_{dksr} \frac{D_{dksr}^{\text{affected-accom}}}{R_{kr}^{\text{accom}}} \leq R_{kr}^{\text{accom}} \quad \forall k, r, s \tag{16}$$

$$\sum_{r=1}^R \chi_{lsr} \leq \chi_{ls0} \quad \forall l, s \tag{17}$$

$$\sum_{r=1}^R \chi'_{ksc} \leq \chi'_{ksc0} \quad \forall k, s \tag{18}$$

$$\sum_{l \in \text{FR}} \sum_{r=1}^R \zeta_{dlrs} + \sum_{i \in \text{FR}} \zeta_{diso} = 1 \quad \forall d, s \tag{19}$$

$$\sum_{k \in \text{AD}} \sum_{r=1}^R \zeta'_{dkrs} + \sum_{k \in \text{AR}} \zeta'_{dks0} = 1 \quad \forall d, r \tag{20}$$

$$\Lambda_{dls} \leq M \zeta_{dlrs} \quad \forall d, l, s, r \tag{21}$$

$$\Lambda'_{dks} \leq M \zeta'_{dkrs} \quad \forall d, k, s, r \tag{22}$$

$$\zeta_{dlrs} \leq \chi_{lrs} \quad \forall l, d, r, s \tag{23}$$

$$\zeta'_{dkrs} \leq \chi'_{krs} \quad \forall k, d, r, s \tag{24}$$

$$\sum_{h=1}^H \Lambda''_{dhs} = D_{ds}^{\text{critical}} \quad \forall d, s \tag{25}$$

$$\sum_{l \in \text{FD} \cup \text{FR}} D_{ds}^{\text{outpatient}} = \sum_{l \in \text{FD} \cup \text{FR}} \zeta_{dlrs} \times \Lambda_{dls} \quad \forall d, r, s \tag{26}$$

$$\sum_{k \in \text{AD} \cup \text{AR}} D_{ds}^{\text{evac}} = \sum_{k \in \text{AD} \cup \text{AR}} \zeta'_{dkrs} \times \Lambda'_{dks} \quad \forall d, r, s \tag{27}$$

$$\chi_{lrs}, \chi'_{krs}, \zeta_{dlrs}, \zeta'_{dkrs}, \psi_{ekrs} \in \{0, 1\} \quad \forall d, r, s, l, k, e \tag{28}$$

$$\Lambda_{dls}, \Lambda'_{dks}, \Lambda''_{dhs}, \gamma_{vdlrs}, \gamma'_{vdks}, \gamma''_{vdhs}, \gamma_{vekrs}, \omega_{kctrs}, \Gamma_{ekcts}, \Gamma_{kcts} \geq 0, \text{ integer } \forall d, r, s, l, k, c, t, h, e, v \tag{29}$$

The objective function as expressed in Equation (5), represented as the sum of G1, G2, G3, and G4, which aims to minimize the total costs associated with humanitarian logistics operations in the aftermath of global warming-induced disasters. This comprehensive minimization problem systematically addresses various critical cost components to ensure an efficient and effective disaster response. The first component of this objective, G1 as shown in Equation (1), specifically targets the cost attributed to casualties at temporary care facilities stemming from global warming impacts. This segment quantifies the expected penalty for the loss of individuals requiring outpatient services. It meticulously considers the probability of failure for initial temporary care centers, represented by care fail for facilities in D, and contrasts this with the successful operation (or replacement by backup facilities) of resilient centers, indicated by (1 – P_{care fail}) for facilities in FR. The allocation variable ζ_{dlrs} signifies the assignment of an affected area to a particular temporary care facility at a given allocation level. Similarly, G2 in Equation (2) addresses the cost incurred due to casualties at temporary accommodation centers, also as a consequence of global warming impacts. This part mirrors the structure of G1, calculating the expected penalty for the loss of evacuees. It accounts for the failure probability of initial temporary accommodation centers, P_{accom fail} for facilities in AD, and the effective functioning of resilient or backup centers, (1 – P_{accom fail}) for facilities in AR. The allocation variable ζ' denotes the assignment of an affected area to a temporary accommodation center.

The third component, G₃ in Equation (3), consolidates all transportation-related costs across various routes and scenarios. This extensive section covers four distinct aspects of logistical movement. It includes the costs associated with transporting individuals from affected areas to temporary accommodation centers, from affected areas to temporary care facilities, and from affected areas to hospitals. Furthermore, it incorporates the costs of transporting commodities from distribution hubs to temporary accommodation centers. Each part is calculated based on the distance between facilities and the number of vehicles deployed, reflecting the operational expenses of the entire relief distribution

network. Finally, G_4 in Equation (4) encompasses two crucial cost categories. The first part represents the expenditures for establishing both temporary care and temporary accommodation facilities. This includes the investment required to set up these critical infrastructure points, considering various allocation levels and scenarios. The second part of G_4 is the total weighted shortage cost of commodities. This directly addresses the second objective function of the model, aiming to minimize the unmet demand for essential supplies. The inclusion of the priority coefficient ψ_c within this term ensures that commodities deemed more urgent or critical are prioritized, thereby mitigating the impact of shortages on the most vital relief supplies. In essence, the objective function comprehensively captures the financial repercussions of disaster response, ranging from the tragic costs of human casualties and the operational costs of logistics and infrastructure establishment to the critical cost of unmet humanitarian needs. By minimizing this combined function, the model seeks to optimize resource allocation and operational planning in a manner that is both economically efficient and responsive to human welfare in the face of global warming challenges.

The third component, G_3 in Equation (3), consolidates all transportation-related costs across various routes and scenarios. This extensive section covers four distinct aspects of logistical movement. It includes the costs associated with transporting individuals from affected areas to temporary accommodation centers, from affected areas to temporary care facilities, and from affected areas to hospitals. Furthermore, it incorporates the costs of transporting commodities from distribution hubs to temporary accommodation centers. Each part is calculated based on the distance between facilities and the number of vehicles deployed, reflecting the operational expenses of the entire relief distribution network. Finally, G_4 in Equation (4) encompasses two crucial cost categories. The first part represents the expenditures for establishing both temporary care and temporary accommodation facilities. This includes the investment required to set up these critical infrastructure points, considering various allocation levels and scenarios. The second part of G_4 is the total weighted shortage cost of commodities. This directly addresses the second objective function of the model, aiming to minimize the unmet demand for essential supplies. The inclusion of the priority coefficient ψ_c within this term ensures that commodities deemed more urgent or critical are prioritized, thereby mitigating the impact of shortages on the most vital relief supplies. In essence, the objective function comprehensively captures the financial repercussions of disaster response, ranging from the tragic costs of human casualties and the operational costs of logistics and infrastructure establishment to the critical cost of unmet humanitarian needs. By minimizing this combined function, the model seeks to optimize resource allocation and operational planning in a manner that is both economically efficient and responsive to human welfare in the face of global warming challenges.

The model also incorporates a series of constraints to accurately represent the complexities of post-disaster humanitarian logistics under global warming impacts as seen above. Constraint (6) governs the flow of crucial relief supplies within temporary accommodation centers, stipulating that the total quantity of commodities received from distribution hubs, combined with any existing shortages, must meet or exceed the specified demand. Complementing this, constraint (7) permits the storage of goods within a temporary accommodation center only if that facility has been established. The capacity limitations of healthcare infrastructure are addressed by constraint (8), which restricts the number of critically injured individuals admitted to any hospital to its maximum patient intake. Similarly, constraint (9) ensures that the outflow of commodities from each distribution center does not surpass its designated capacity. Commodity requirements for each scenario and time period are formalized by constraint (10), where the demand for each type of supply is derived by multiplying its consumption coefficient by the number of affected individuals.

Transportation capabilities are meticulously managed through several constraints. Constraint (11) sets the upper limit for transferring non-critically injured individuals from affected zones to temporary care facilities, ensuring it remains within the carrying capacity of available vehicles. Analogously, constraint (12) imposes a similar vehicle capacity limit for moving displaced persons from affected areas to temporary accommodation centers. For critically injured individuals, constraint (13) regulates their transport from affected zones to hospitals, again constrained by vehicle capacity. The movement of relief commodities is specifically addressed by constraint (14), which dictates that the volume of supplies transported from distribution centers to accommodation centers cannot exceed the collective capacity of the vehicles operating on these routes.

Geographical allocation and facility establishment are also critical. Constraint (15) permits the assignment of affected areas to temporary care facilities only when the distance between them falls within the facility's designated coverage range. A parallel condition is applied by constraint (16) for the allocation of affected areas to temporary accommodation centers, based on their respective coverage distances. Furthermore, constraints (17) and (18) enforce a hierarchical establishment process: backup care and accommodation centers, respectively, can only be set up if their corresponding initial facilities (at allocation level $r = 0$) are already in place. Universal access to care and shelter is ensured through constraints (19) and (20). Constraint (19) mandates that every affected area, across all allocation levels, must be assigned to at least one resilient temporary care center; once assigned to such a facility, further allocations to other centers cease. This means each affected area must be linked to either an initial or a backup care facility. A similar principle applies to accommodation centers under constraint (20), guaranteeing that all affected areas are allocated to at least one resilient temporary accommodation center, halting further assignments once this condition is met. The operational flow between facilities is contingent on established allocations. Constraint (21) dictates that the movement of individuals between an affected area and a temporary care center can only occur if that area has been explicitly assigned to that specific care center at a designated allocation level. Likewise, constraint (22) enforces this condition for the flow between an affected area and a temporary accommodation center. Prioritization of establishment over allocation is emphasized by constraints (23) and (24): a temporary care center must be established before any affected area can be allocated to it, and the same rule applies to temporary accommodation centers. Finally, full coverage for essential needs is secured. Constraint (25) ensures that all critically injured individuals from each affected area are successfully transferred to hospitals. Constraint (26) guarantees that all non-critically injured individuals from affected areas are directed to temporary care centers. Similarly, constraint (27) ensures that all individuals displaced by global warming impacts from each affected area are transported to temporary accommodation centers. The nature of the decision variables, whether binary or non-negative integers, is defined by constraints (28) and (29), respectively.

SOLUTION METHODOLOGY

In this research, a multi-faceted approach is employed to tackle the optimization problem. Three distinct methodologies are utilized for solution generation and analysis. The first method is the Non-Dominated Sorting Genetic Algorithm II (NSGA-II). The second strategy involves the epsilon-constraint technique. The third approach is a Modified Multi-Objective Particle Swarm Optimization (MMOPSO), which integrates elements of the standard Particle Swarm Optimization (PSO) with two localized search procedures.

4.1 NSGA-II Implementation

NSGA-II stands as a prominent and widely adopted metaheuristic for multi-objective optimization, often serving as a foundational benchmark for evaluating other algorithmic advancements in this domain. Its robust performance has led to numerous successful applications in various fields in recent years.

4.1.1 Chromosomal Encoding

The model employs a multi-segment chromosomal representation, structured uniquely for each scenario and time period. One segment is dedicated to indicating the operational status of temporary care facilities, encoded as a binary

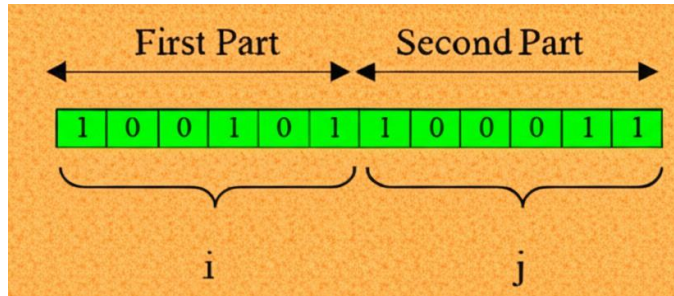


Figure 1: 1-dimensional chromosomal representation

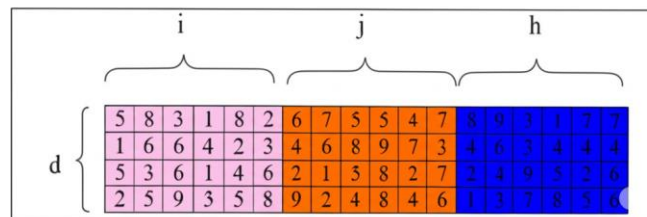


Figure 2: 2-dimensional chromosomal representation for optimized allocation of wounded persons

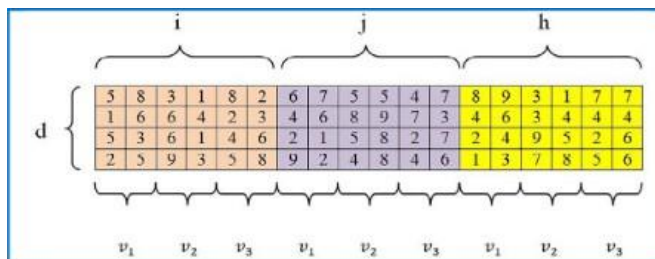


Figure 3: 2-dimensional chromosomal representation for the number of vehicles

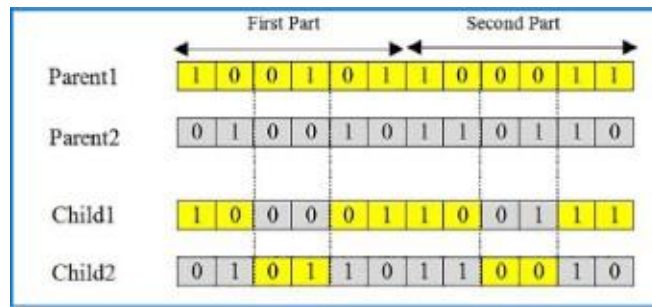


Figure 4: Double-point crossover

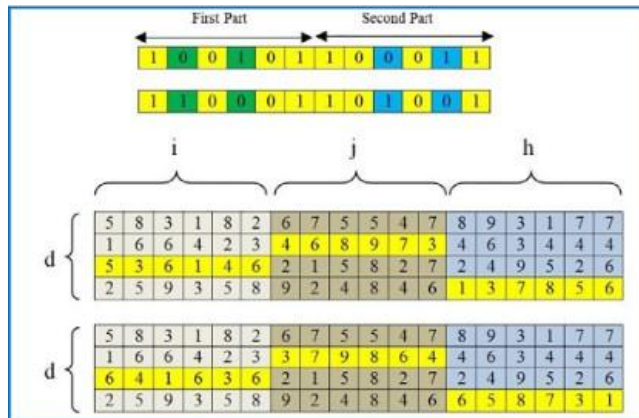


Figure 5: Mutation operator

Matrix where a value of 1 signifies activation and 0 denotes non-activation. A similar binary matrix constitutes another segment, determining the operational status of temporary accommodation centers, with 1 for active and 0 for inactive. A separate, two-dimensional chromosomal structure is utilized to manage the allocation of injured individuals. This chromosome is divided into three sections, each corresponding to the assignment of casualties to temporary care centers, temporary accommodation centers, and hospitals. The numerical values within each gene of this representation directly reflect the quantity of injured individuals directed to these respective facilities. Furthermore, a third distinct two-dimensional chromosome is designed to manage vehicle deployment. This chromosome, also comprising three parts, dictates the number of vehicles dispatched from affected areas to temporary care centers, temporary accommodation centers, and hospitals. The model distinguishes between three types of vehicles, labeled v1, v2, and v3.

4.1.2 Genetic Operators

The **crossover operator** is a hybrid process executed in three stages. Initially, two chromosomes are chosen at random. Subsequently, a merging point within the chromosome string is randomly selected. Finally, the segments of the two chromosomes are exchanged based on the chosen merging point. A Double-point crossover technique is specifically applied in this operation. The **mutation operator** varies depending on the chromosome’s dimensionality. For single-dimensional chromosomes, a randomly selected gene within a chromosome is replaced with an alternative gene. For two-dimensional chromosomes, a row is randomly chosen, and the order of its genes is inverted to introduce variation.

Table 1: Parameters of the MMOPSO algorithm.

Number of iteration	$T_{\max} = 500$
Number of particles	$N_{\alpha} = 50$
Inertia weight	$C_0 = 0.6$
Cognitive (local) accelerator constant	$C_1 = 0.6$
Social (global) accelerator constant	$C_2 = 0.7$

4.1.3 Evaluation Criteria

In the context of the NSGA-II methodology, the effectiveness of each potential solution for the multi-objective model (equations 1-26) is assessed through a fitness function derived directly from the primary objective functions (equations 1 and 2). It is important to note that the ultimate fitness score for each non-dominated solution within the NSGA-II framework is determined through a specialized non-dominated sorting procedure.

4.1.4 Managing Constraints

The various operational constraints (equations 2-26) embedded within the proposed model are addressed through the application of a penalty function approach. Should the NSGA-II algorithm generate a solution that violates any of these constraints during its iterative search, a predefined penalty is imposed on the corresponding objective function values, effectively discouraging infeasible outcomes.

4.2 Epsilon-Constraint Approach

The epsilon-constraint method stands as a highly recognized and effective technique for navigating multi-objective optimization challenges. This methodology is particularly adept at generating the complete Pareto Front, which represents the set of optimal trade-off solutions. A pronounced strength of the epsilon-constraint method, distinguishing it from other multi-objective optimization techniques like the weighted sum approach, lies in its robust performance within non-convex solution spaces, where alternative methods often prove less effective. Recent studies have demonstrated its successful application across various domains. In essence, this technique operates by optimizing one primary objective while simultaneously imposing an upper permissible bound (epsilon) on the values of all other objectives. This process is iteratively performed to map out the entire Pareto frontier, such that;

$$\begin{aligned}
 \min \quad & g_1(w) \leq \epsilon_1 \quad \forall w \in W \\
 & g_2(w) \leq \epsilon_2 \\
 & \vdots \\
 & g_n(w) \leq \epsilon_n
 \end{aligned} \tag{30}$$

4.3 Modified Multi-Objective Particle Swarm Optimization (MMOPSO)

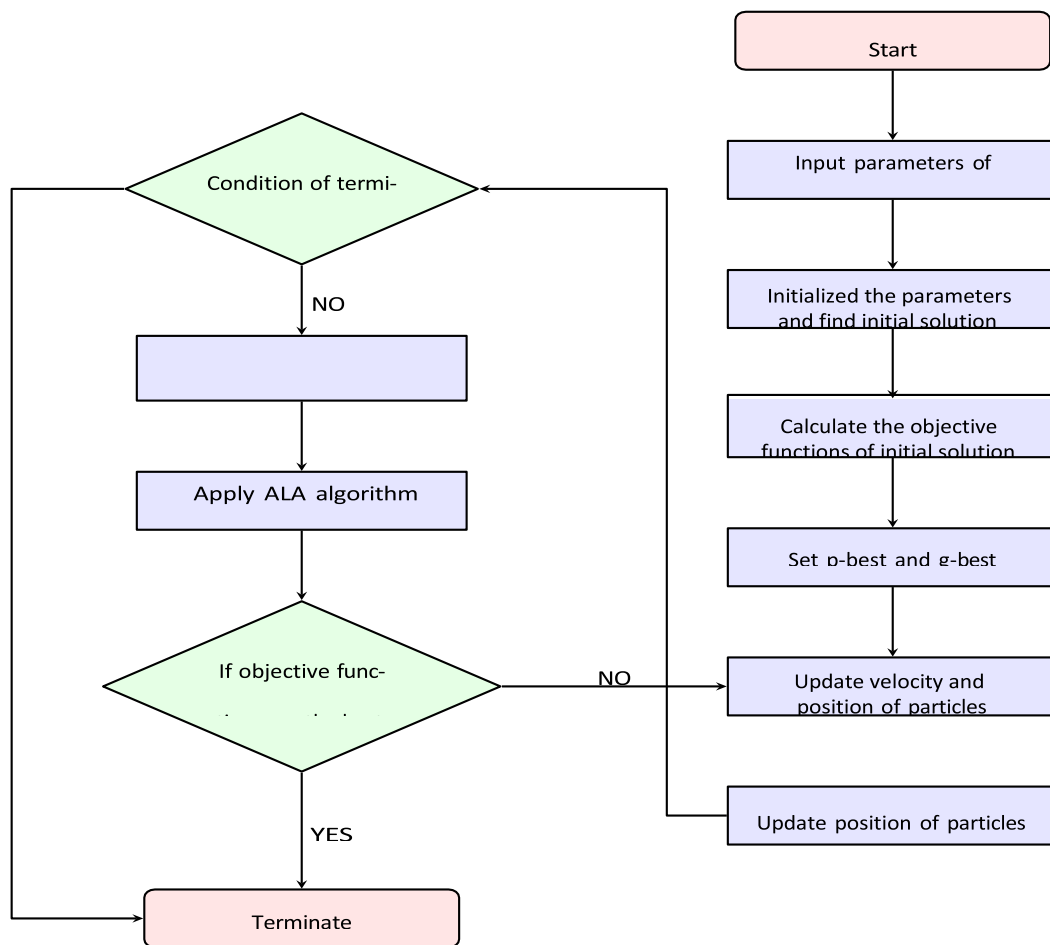
Building upon the Multi-Objective Particle Swarm Optimization (MOPSO) technique initially proposed by Moore and Chapman [24] for tackling multi-objective problems, this study introduces a Modified Multi-

Objective Particle Swarm Optimization (MMOPSO) variant. An interesting characteristics of the MOPSO algorithm is its capacity to retain not only the overall Pareto front solutions but also the localized Pareto solutions for each individual particle. This mechanism ensures that each particle’s optimal position is preserved until a superior solution is discovered. The movement trajectory of particles, encapsulated by their velocity vector, is governed by three primary components: an inertia factor, a global accelerator, and a local accelerator. The local accelerator is influenced by the particle’s current position and its personal Pareto front, effectively representing its historical best location. Inertia is defined by the particle’s velocity from the preceding iteration. The global accelerator, conversely, is shaped by the particle’s current position and the collective Pareto front of the swarm. For the purpose of this research, the particle movement mechanism is formally defined by the following equation:

$$Z_t = (D_0 \cdot Z_{t-1}) + (D_1 \cdot \text{rand}(\text{PPZ}_t - Z_t)) + (D_2 \cdot \text{rand} \cdot (\text{PGZ}_t - Z_t)) \tag{31}$$

4.4 Heuristic Approach for Facility Location and Allocation

An alternative heuristic algorithm, developed by Cooper [8], is employed for localized search within location-allocation problems. This algorithm is instrumental in determining the optimal placement of distribution centers, temporary accommodation centers, and temporary care centers, as well as managing the assignment of injured and displaced individuals to these facilities following a disaster. The algorithm functions by decomposing the larger problem into



Repeat steps below

Step 0: Select m locations using the clustering approach as the initial solution

Phase 1: Implement the EH algorithm.

Step 1: Allocate each affected area to the nearest potential location

Step 2: Look for a pair of potential locations (one location to insert and another location to remove)

Step 3: If this pair of places is found, repeat the steps 1 and 2 until you reach to the stopping criterion, or else, there will not be any improvement in the solution and you have to go to Phase 2.

Phase 2: Implement the Cooper algorithm (ALA)

Step 1: Allocate each affected area to the nearest potential location

Step 2: Keep constant the current allocation of the affected area and relocate the potential locations by solving the m single location problems (using the Weiszfeld method)

Step 3: Repeat Steps 1 and 2 until there is no further improvement.

Smaller subsets, subsequently identifying the optimal single-source location for each subset using an exact location methodology. The precise optimal location for each facility is computed using Weiszfeld's approach [35], mathematically expressed as:

$$Z_{k+1} = \frac{\sum_{i=1}^n \frac{v_i Z_i}{\sqrt{(Z_i - Z_k)^2 + (Y_i - Y_k)^2}}}{\sum_{i=1}^n \frac{v_i}{\sqrt{(Z_i - Z_k)^2 + (Y_i - Y_k)^2}}} \quad (32)$$

The iterative adjustment of facility coordinates is further defined by the following equation:

$$Y_{k+1}^- = \frac{\sum_{i=1}^n \frac{v_i Y_i}{\sqrt{(Z_i - Z_k)^2 + (Y_i - Y_k)^2}}}{\sum_{i=1}^n \frac{v_i}{\sqrt{(Z_i - Z_k)^2 + (Y_i - Y_k)^2}}} \quad (33)$$

The convergence criterion for this iterative process is satisfied when the coordinates stabilize between successive iterations, as expressed by:

$$Y_{k+1}^- = Y_k^- \quad Z_{k+1} = Z_k^- \quad (34)$$

Here, (z_i, y_i) denotes the spatial coordinates of source i, and v_i represents its associated weighting or priority level.

4.5 Exchange Heuristic (EH)

The Exchange Heuristic (EH) algorithm, a local search method developed by Teitz and Bart [34], is employed for solving discrete space location-allocation problems. This algorithm systematically searches for optimal location pairings in each iteration. In the context of this research, affected areas, denoted by d , serve as potential sites for establishing facilities. The spatial separation between a candidate location v and an affected area d is given by $\text{dist}(v, d)$. A solution, represented by Z , signifies the selected facility locations. Each affected area d is assigned to its closest candidate location, aiming to minimize $\text{dist}(v, d)$. This closest location is identified as $\psi_1(d)$. The algorithm also requires identifying the second nearest location, termed $\psi_2(d)$. For brevity, the distances to the first and second nearest locations are referred to as $\text{dist}_1(d)$ and $\text{dist}_2(d)$, respectively. Locations considered for potential removal are designated as VR (where $v_r \in Z$, indicating they are currently part of the chosen set of facilities). For every possible pairing of a candidate location for removal (v_r) and a candidate location for insertion (v_i), the potential benefit from such a relocation is quantitatively assessed. This relocation benefit is calculated using Equation (35).

$$\begin{aligned}
 \text{Benefit}(v_i, v_r) = & \sum_{d \in D} \max\{0, [\text{dist}_1(d) - \text{dist}(d, v_i)]\} \\
 & - \sum_{\substack{d: \psi_1(d) = v_r \\ \text{dist}(d, v_i) < \text{dist}_2(d)}} [\text{dist}_2(d) - \text{dist}_1(d)] \\
 & + \sum_{d: [\psi_1(d) = v_r] \cap [\text{dist}(d, v_i) < \text{dist}_2(d)]} [\text{dist}_2(d) - \max\{\text{dist}(d, v_i), \text{dist}_1(d)\}]
 \end{aligned} \tag{35}$$

This calculated benefit comprises three distinct components. The first component, termed Gain(v_i)

\sum

$d \in D$

$\max\{0, [\text{dist}_1(d) - \text{dist}(d, v_i)]\}$, represents the cumulative improvement achieved if v_i were to be added to the current set of facilities, irrespective of which existing facility might be removed. The second component of the equation, Loss(v_r) =

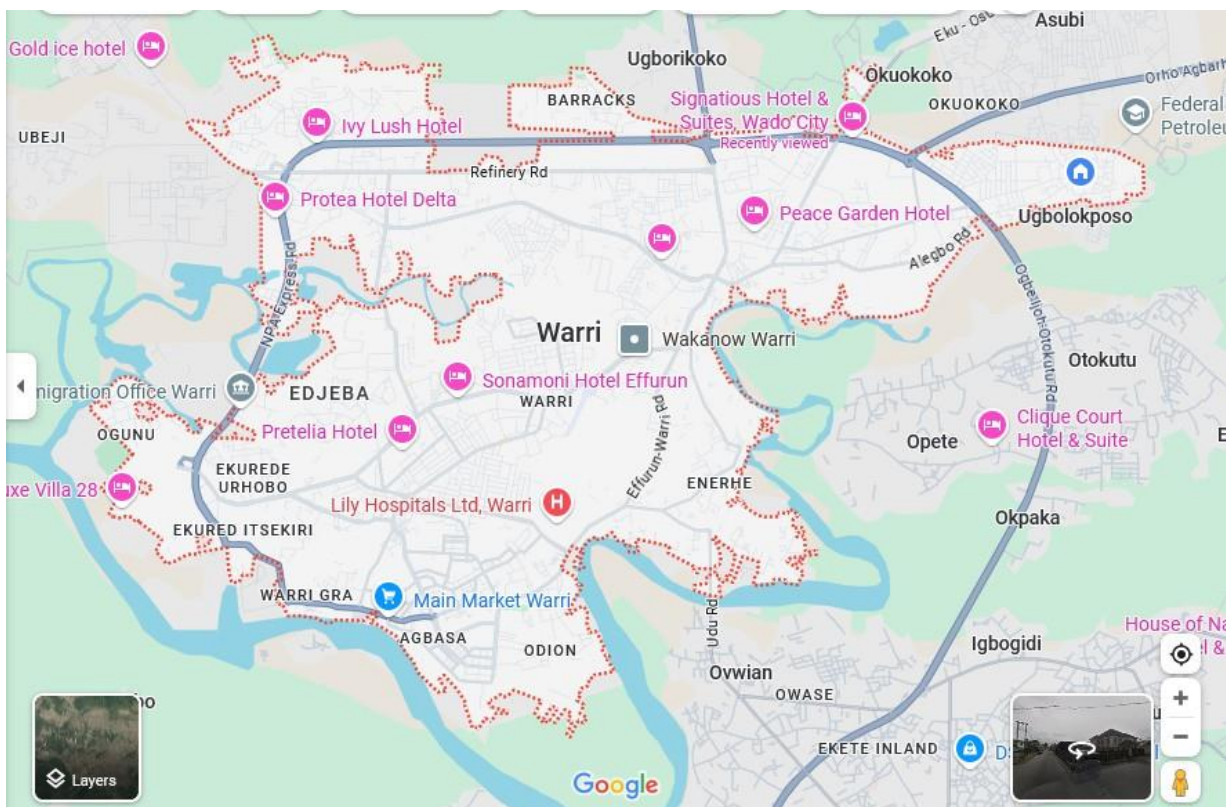


Figure 7: Map of Warri and Environs, showing flood-prone areas and locations of critical facilities: H (Hospitals/Medical Posts), R (Relief Distribution Centers), C (Temporary Care Centers), and A (Temporary Accommodation Centers)

$d: \psi_1(d)=v_r$ [$\text{dist}_1(d) - \text{dist}_1(d)$], quantifies the increase in solution cost or degradation in quality resulting from the elimination of facility v_r . Finally, the third component, $\text{Adjustment}(v_i, v_r) = d: [\psi_1(d)=v_r] \cap [\text{dist}(d, v_i) < \text{dist}_2(d)] [\text{dist}_2(d) - \max\{\text{dist}(d, v_i), \text{dist}_1(d)\}]$, captures the intricate combined effect of swapping v_r with v_i on the affected areas that were previously primarily served by v_r .

REAL WORLD APPLICATION

The city of Warri, located in Delta State, Nigeria, is considered highly prone to recurrent annual flooding, particularly during the rainy season. Given its low-lying topography, extensive network of creeks and rivers, inadequate drainage infrastructure, and the influence of heavy rainfall and tidal surges, flood events can lead to significant and often irreparable damages and losses to infrastructure, livelihoods, and lives. The broader Warri and its environs encompass various communities and local government areas highly susceptible to inundation. For this case study, the critical period for immediate rescue and relief operations following a major flood event is considered to be 72 hours, divided into two 36-hour periods for strategic planning

Fig.7 illustrates a conceptual map of Warri and its environs, highlighting key areas and the distribution of crucial facilities for flood response. This includes existing hospitals and primary healthcare centers (H points), designated relief distribution centers (R points), potential locations for temporary care centers for the injured and displaced (C points), and sites for establishing temporary accommodation centers for evacuees (A points). In line with many disaster management studies, the affected areas are delineated based on existing urban and community divisions. For instance, research on flood resilience often defines affected areas as specific wards, communities, or local government areas that experience significant inundation and require intervention. Therefore, in this research, different communities and urban segments within Warri and its environs are considered as demand points. Given the diverse and sprawling nature of Warri and its surrounding communities, we consider 15 distinct, flood-prone areas as affected zones, each representing an associated demand point for aid. Table 3 outlines various flood scenarios defined for Warri and its environs, along with their estimated probabilities of occurrence. These scenarios reflect different primary drivers of flooding in the region. Table 4 illustrates a set of potential locations for the establishment of distribution centers for

Table 3: Different flood scenarios for Warri and Environs, and their estimated probability of occurrence.

Flood Scenario	Intense Rainfall		River Overflow		Coastal Surge		Combined Event	
Severity of Occurrence	Moderate		High		Moderate to High		Very High	
Time of Occurrence	Day	Night	Day	Night	Day	Night	Day	Night
Probability of Occurrence	0.2500	0.1500	0.1000	0.0800	0.0700	0.0500	0.1800	0.1200
Percentage of Affected Area	15%		35%		20%		60%	

Table 4: Set of potential locations for the establishment of relief distribution centers in Warri and Environs.

No	Name of the Area/Facility
e1 1	Warri City Stadium Grounds
e2 2	Enerhen Junction Community Hall
e3 3	Effurun Market Area (Open Space)
e4 4	PTI Conference Centre (Grounds)
e5 5	Okere-Urhobo Town Hall
e6 6	Agbarho Main Market Square
e7 7	Ugbomro Community Civic Centre
e8 8	Ekpan Community Field
e9 9	Osubi Airport Road Industrial Area (Warehouses)
e1 0	Federal University of Petroleum Resources (FUPRE), Effurun campus (for wider area support)
e1 1	Army Barracks Ground (if accessible for civilian use)
1 1	
e1 1	Public School Compounds (e.g., larger ones during holidays)
2 2	

relief commodities within Warri and its environs. These locations are strategic points with reasonable access and space. These centers can be established at small, medium, or large scales, each possessing distinct capacities and associated construction/setup costs. The optimal type and scale of the constructed distribution center are determined by the proposed model. Table 5 identifies candidate locations for temporary care centers, which are crucial for providing

Table 5: Candidate locations for temporary care centers for flood victims in Warri and Environs.

No.	Name of the Area/Facility
i1 1	Federal Medical Centre (FMC) Annex (if not directly impacted)
i2 2	Primary Health Care Center (e.g., within a larger un-flooded community)
i3 3	Selected Large Church/Mosque Halls
i4 4	Some Accessible School Gymnasiums/Halls
i5 5	Community Sports Complexes (e.g., in Ughelli, closer if Warri completely submerged)

immediate medical attention and shelter to injured or vulnerable flood victims. To minimize the time spent serving affected individuals, transferring them to existing care centers is possible both directly from affected areas and via designated transfer points. Table 6 presents potential locations for establishing temporary accommodation centers,

Table 6: Potential locations for the establishment of temporary accommodation centers for displaced persons in Warri and Environs.

No	Name of the Area/Facility	No	Name of the Area/Facility
1	Warri Stadium Complex	5	Ugborikoko Secondary School (large compound)
2	Petroleum Training Institute, Effurun (Student Hostels)	6	Federal University of Petroleum Resources (FUPRE) Stadium
3	Government Technical College, Effurun (Grounds/Halls)	7	PTI Conference Center Hostel
4	Large Hotel Conference Halls (if leased for emergency)	8	Naval Base Barracks (if allocated for civilian use)

which are vital for housing displaced populations for extended periods during and after major flood events. Table 7 details critical information such as the priority of meeting demand and the associated costs for supplying each type of relief commodity essential during flood response operations. It is assumed that inventory maintenance costs and supply costs for the post-disaster phase are consistent with the pre-disaster phase for planning purposes.

Table 7: Parameters required for supplying various relief commodities during flood response.

Commodity	Type of the commodity	Priority	Volume (m3)	Weight (kg)	Transportation cost (\$/km/unit)	Cost of shortage (103\$/unit)
C1	Food Packs (Dry Rations)	0.95	0.01	5	0.08	0.09
C2	Bottled Water (5 Litre)	0.98	0.005	5	0.06	0.12
C3	Mosquito Nets	0.80	0.002	0.5	0.05	0.03
C4	Hygiene Kits (Soap, Sanitary Pads)	0.75	0.003	1	0.07	0.04
C5	First Aid Kits	0.90	0.001	0.2	0.10	0.08
C6	Life Jackets/Buoyancy Aids	0.60	0.05	2	0.12	0.06
C7	Tarpaulins/Shelter Sheets	0.85	0.03	3	0.09	0.07

It is further assumed that suppliers can utilize only 60% of their normal capacity during the immediate post-flood phase due to transportation challenges and disruptions. The flood response network is assumed to have access to 50 various transportation vehicles (e.g., trucks, smaller boats for inundated areas). Each existing healthcare facility (hospital or well-equipped clinic) is assumed to have a limited number of rapid response vehicles or boats (e.g., 5 per facility) for deploying to affected areas for initial assessment and patient transfer.

Table 8: Types of relief distribution centers based on scale, capacity, and establishment cost.

Type of Center	Scale	Capacity (Units of Aid/Day)	Estimated Establishment Cost (103\$)
Type 1	Small	1,500	50
Type 2	Medium	5,000	150
Type 3	Large	15,000	400

Table 8 identifies the different types of distribution centers in terms of their scale, operational capacity, and estimated establishment costs, which are crucial decision variables for resource allocation.

Table 9: Parameters related to the establishment of flood relief distribution centers in Warri and environs.

Estimated Establishment Cost (103\$)	Capacity (Aid Units/Day)	Scale	Distribution Center Type
120	2500	Small	D1
180	5000	Medium	D2
280	10000	Large	D3

Table 10: Tuned parameters for the NSGA-II algorithm for flood relief optimization.

Mutation rate	Crossover rate	Population size	Max iterations
0.06	0.5	100	120

The epsilon-constraint method, tailored for multi-objective optimization, is implemented using GAMS 24.9.1 software. For metaheuristic approaches, MATLAB R2017a v9.2.0.53 software is utilized to code the NSGA-II and MMOPOS algorithms. The computational environment for these simulations includes a laptop equipped with 8 GB RAM, an Intel Core i5 7200U processor, and running Win10 64bit. The NSGA-II algorithm, a prominent multi-objective evolutionary algorithm, is applied with various configurations of its parameters. Table 10 details the optimal configuration of parameters derived through calibration and used in this study for the NSGA-II algorithm.

5.1 Performance Evaluation of NSGA-II and MMOPOS Algorithms for Flood Relief Optimization

In this section, to rigorously evaluate the performance of the proposed solution approaches for optimizing flood relief operations in Warri and its environs, five key metrics are employed:

Spacing (SM): This metric quantifies the standard deviation of the distances between consecutive solutions on the Pareto front [41], indicating the uniformity of the solution spread.

Mean Ideal Distance (MID): MID measures the convergence rate of the generated Pareto fronts towards an ideal point (0, 0) in the objective space [42], reflecting how close the solutions are to the optimal trade-off.

Convergence: Assesses the algorithm’s ability to consistently find solutions that are close to the true Pareto front.

Hypervolume Indicator (HV): A comprehensive metric that measures the volume of the objective space dominated by the Pareto front, providing insights into both convergence and diversity.

Statistical Test Analysis: Used to determine the statistical significance of performance differences between the algorithms.

5.2 Spacing Metric (SM)

The Spacing metric (SM) quantifies the uniformity of the distribution and spread of the non-dominated set of solutions along the Pareto front. It is calculated using the following formula:

$$SM = \frac{1}{n-1} \sum_{i=1}^{n-1} (d_i - d^-)^2 \tag{36}$$

Here, d_i represents the Euclidean distance between two adjacent Pareto solutions in the objective space, and d^- denotes the average Euclidean distance among all adjacent solutions. A smaller SM value signifies a lower dispersion of Pareto points, indicating a more evenly distributed and well-spread Pareto front. Ideally, when SM approaches zero, the distances between all adjacent solutions on the Pareto front are approximately equal.

5.3 Mean Ideal Distance (MID)

The Mean Ideal Distance (MID) metric is utilized to assess the proximity of the generated Pareto solutions to the ideal point in the objective space [12]. The MID index is calculated as follows:

$$MID = \frac{1}{n} \sum_{i=1}^n \left(\frac{(f_{1i} - f_1^*)^2}{R_1^2} + \frac{(f_{2i} - f_2^*)^2}{R_2^2} \right) \tag{37}$$

In this equation, n refers to the total number of Pareto solutions obtained. f_{ji} represents the value of the j -th objective for the i -th solution in the Pareto frontier. f^* denotes the ideal (maximum or minimum, depending on the objective type) value of the j -th objective observed among all solutions in the Pareto frontier. R_j represents the range of the j -th objective. According to this definition, an algorithm that yields a lower value for the MID demonstrates superior convergence and performance, as its solutions are closer to the ideal trade-off point.

To thoroughly evaluate the effectiveness of the proposed solution approaches in the context of flood relief logistics, the following experimental methodology has been adopted. Initially, a set of ten random small and medium-scale test instances, representative of flood scenarios in Warri and its environs, are generated. The specific configurations and characteristics of these random instances are detailed in Table 11. All these generated instances are then solved using the epsilon-constraint method, NSGA-II, and MMOPOS algorithms. The performance evaluation metrics, specifically MID, SM, and CPU Time, are computed for all solution approaches across these instances and are presented in Table 12. An evaluation of the three algorithms on small and medium-sized problems reveals the strong performance of the MMOPSO method when measured by the Mean Ideal Distance (MID) metric. MMOPSO achieved an average MID of 3.921, which is a notable improvement over NSGA-II's score of 4.012. Furthermore, its result was highly competitive with the ϵ -constraint method (mean MID of 3.889), differing by a marginal 0.032. These findings confirm that, based on the MID criterion, the MMOPSO algorithm is superior to NSGA-II.

The mean value of SMs for the ϵ -constraint method, NSGA-II, and MMOPOS are 0.380, 0.395, and 0.408, respectively. It can be observed that the mean value of SM for the ϵ -constraint method is marginally lower than that of NSGA-II. Furthermore, a difference of 0.028 in the mean MID value is noted in favor of the ϵ -constraint method when compared to MMOPOS. Therefore, based on the SM metric, MMOPOS demonstrates a slightly better performance than NSGA-II. Overall, it can be concluded that the results for MID and SM indicate that the MMOPOS method generally performs slightly better than NSGA-II for small and medium-sized problems. As evidenced by Table 17, the CPU Time for the ϵ -constraint method remains significantly higher, making it less comparable to the more efficient NSGA-II and MMOPOS algorithms for larger problem instances.

Table 11: Dimensions of the flood-response instances used to verify the solution approaches.

Problem number	Problem scale	Affected areas	Temporary accommodation centers	Distribution centers	Healthcare facilities
1	Small	3	1	1	1
2	Small	4	1	2	2
3	Small	5	2	2	3
4	Small	6	2	3	4
5	Small	7	3	3	5
6	Medium	8	3	4	6
7	Medium	9	4	5	6
8	Medium	11	4	5	7
9	Medium	12	5	6	7
10	Medium	13	6	6	8

Table 12: Results of multi-objective performance evaluation metrics for flood-response instance test problems.

	MID	SM	Time (s)	MID	SM	Time (s)
1	2.450	0.375	4	2.580	0.380	4
2	2.290	0.370	35	2.350	0.385	6
3	2.550	0.205	68	2.610	0.210	8
4	2.980	0.220	95	3.050	0.230	12
5	3.320	0.435	310	3.380	0.440	21
6	4.750	0.400	700	4.850	0.410	28
7	4.820	0.415	1600	4.930	0.420	38
8	5.010	0.430	2550	5.080	0.450	45
9	5.180	0.460	5700	5.450	0.475	70
10	5.400	0.490	8900	5.850	0.500	105
Ave	3.805	0.380	2005.9	3.960	0.395	34.7

MMOPOSO		
MID	SM	Time(s)
2.180	0.378	4
2.280	0.380	6
2.570	0.210	7
2.910	0.235	10
3.320	0.450	14
4.810	0.410	18
4.840	0.425	28
5.040	0.440	30
5.220	0.470	35
5.500	0.510	52
3.875	0.408	19.4

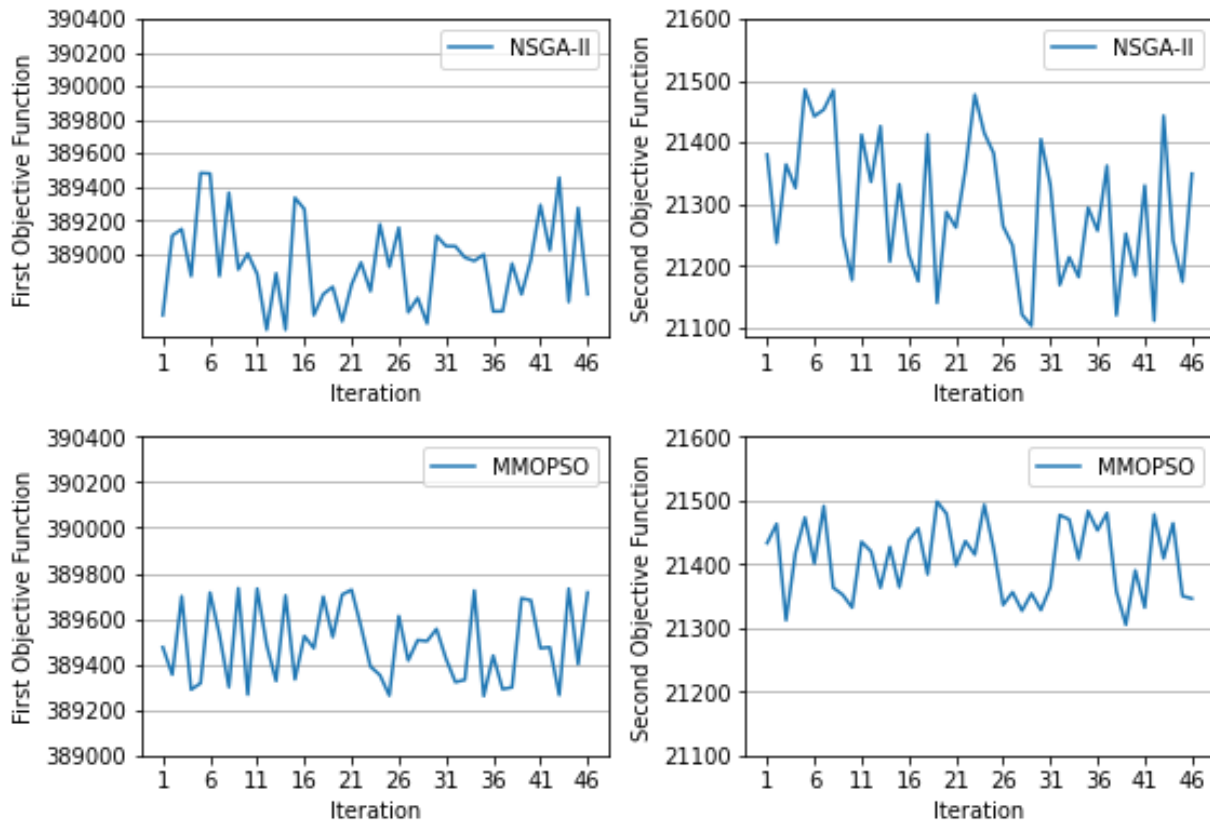


Figure 8: Convergence of the results obtained from NSGA-II and MMOPSO

5.4 Convergence

The convergence of the algorithm’s solutions across multiple runs is a crucial aspect in assessing the overall performance and reliability of the solving algorithms. Consistent convergence confirms that the algorithms are performing as expected and that the generated solutions are robust and acceptable. Based on this criterion, the algorithm employed to solve the model in this study demonstrates suitable performance, yielding acceptable and stable results. A visual representation in Figure 8 illustrates how the solution approaches progressively achieve a stable state for the problem after a manageable number of iterations.

5.5 The Hyper-Volume Metric

A prevalent metric for evaluating the quality of approximate Pareto fronts is the hyper-volume (HV) indicator, initially developed by Zitzler and Thiele [12]. This metric calculates the volume of the objective space that is dominated by a given set of solutions with respect to a predefined reference point. A primary advantage of the HV indicator is its ability to concurrently assess two critical aspects of performance: convergence to the true Pareto front and the diversity of solutions along it. The indicator is formally defined as follows [8]:

$$HV = \text{volume} \int_{i=1}^n v_i \quad (38)$$

Here, the term v_i represents the specific hyper-rectangle (or volume) bounded by the i -th solution and the reference point. In the context of this research, the reference points were determined by aggregating the best solutions found by the epsilon-constraint, NSGA-II, and MMOPSO algorithms across 100 separate runs on all test instances. A larger resulting HV value corresponds to a more effective algorithm. The performance of the MMOPSO and NSGA-II algorithms is compared using the hyper-volume metric in Fig. 9. The figure illustrates that MMOPSO achieved a faster rate of increase in its HV value, indicating superior performance over NSGA-II. Consequently, the set of solutions found by MMOPSO reaches a high-quality, stable state more rapidly than the set produced by NSGA-II.

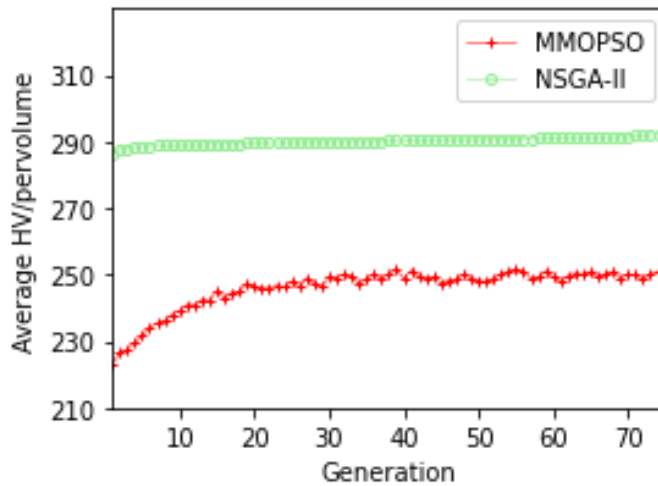


Figure 9: Average hyper volume curve

5.6 Statistical Test Analysis

To ascertain statistically significant distinctions between the proposed algorithmic solutions, an ANOVA (Analysis of Variance) test was employed, as detailed in reference [19]. This section specifically utilizes ANOVA to assess the computational efficiency of the methods by comparing their respective CPU times. The outcomes of the ANOVA analysis are presented in Table 13. As indicated in Table 13, the observed p-value is below 0.05, signifying a statistically significant disparity in the average solution times recorded for the MMOPSO and NSGA-II algorithms.

To further investigate the nature of these differences, Tukey’s Honestly Significant Difference (HSD) post-hoc test was utilized to compare the two solution approaches. This test is applied following the rejection of the null hypothesis in the ANOVA, allowing for a detailed examination of pairwise differences between group means [20]. Specifically, if the ANOVA test identifies a significant overall difference among group means, the Tukey test then proceeds to pinpoint which specific pairs of groups exhibit statistically significant differences.

Table 13: Results of analysis of variance for CPU time.

Source	DF	Adj SS	Adj MS	F Value	P Value
Factor	1	9,533,554,110	9,533,554,110	248.7	0.00
Error	30	1,150,004,800	38,333,495		
Total	31	10,683,558,910			

Table 14: Results of Tukey tests for differences of mean average CPU time.

Difference of means	SE of difference	95% CI	T value	Adjusted P value
NSGA-II-MMOPSO	0.0	453.0 (70,024, 101,770)		18.4 1

Individual confidence level = 95.0%

Table 14 presents the outcomes of the Tukey’s Honestly Significant Difference (HSD) test. The p-value, being above 0.05, suggests no statistically significant difference in the mean CPU time performance. However, it is observed that the MMOPSO approach demonstrates superior CPU time performance, exhibiting a lower mean and standard deviation compared to NSGA-II. Based on the comprehensive statistical analysis and the results from the multi-objective performance evaluation metrics, both NSGA-II and MMOPSO algorithms demonstrate satisfactory performance.

5.7 Comparative Analysis

Given that the specific case study involves a substantial number of components, including 11 hospitals, 10 relief distribution centers, 4 potential temporary care center sites, and 8 potential temporary accommodation center sites, it can be classified as a large-scale optimization problem. The computational results obtained from solving this case

Table 15: Results of multi-objective evaluation metrics for case study

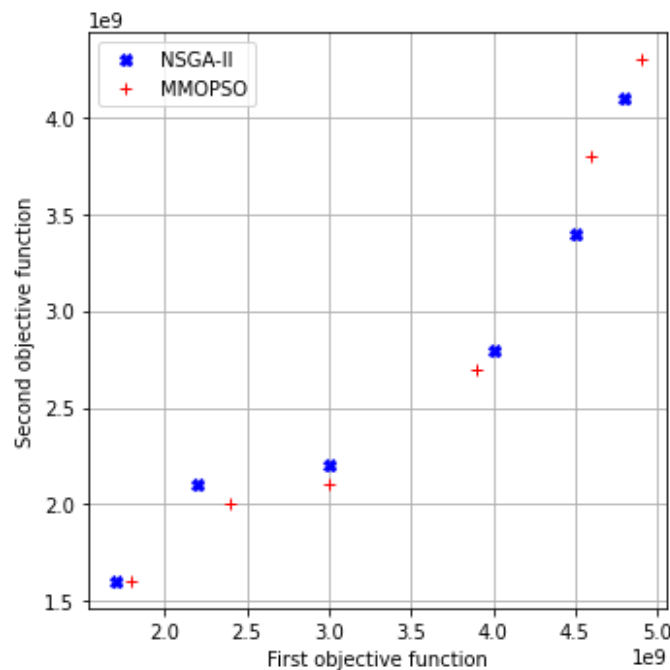
No.	NSGA-II		MMOPSO		Time(s)	
	MID	SM	MID	SM		
1	0.54	0.63	136	0.45	0.59	45
2	0.59	0.65	138	0.48	0.60	47
3	0.60	0.64	135	0.49	0.60	48
4	0.62	0.65	134	0.50	0.59	47
5	0.60	0.64	133	0.54	0.57	48
6	0.61	0.65	135	0.52	0.58	49
7	0.56	0.65	136	0.65	0.60	48
8	0.62	0.65	138	0.63	0.61	51
9	0.59	0.64	137	0.64	0.60	49
10	0.58	0.67	139	0.49	0.56	50
Ave	0.60	0.65	136	0.55	0.57	48.3

study are detailed below: Table 13 provides the values for the MID (Mean Ideal Distance) and SM (Spread Metric) indicators, along with the solution time for the case study. An examination of Table 15 reveals that the average MID value for the MMOPSO method is lower than that of NSGA-II. This indicates that the MMOPSO algorithm achieved a better performance in terms of the MID metric. Similarly, the average SM value for the MMOPSO method is also lower than that of NSGA-II, suggesting that MMOPSO outperformed NSGA-II based on the SM metric as well. Fig. 10 illustrates the optimal values of the Pareto front. The solutions obtained by the NSGA-II approach are represented by blue points, while those from the MMOPSO method are shown as red points. The initial five data points correspond to Pareto solutions for small-scale problem instances, whereas the subsequent five points represent solutions for medium-scale problems. A clear separation or "gap" is visible between these two sets of solutions in the figure, bifurcating the Pareto points into two distinct categories, each comprising five points. This demarcation

arises due to the transition from small-scale to medium-scale problem solutions. As depicted in Fig. 10, for small-scale problems, the average Pareto frontiers are (2,204.73, 1,234,464,000) for MMOPSO and (2,677.75, 1,768,128,000) for NSGA-II, where X and Y denote the first and second objective functions, respectively. For medium-scale problems, the average Pareto frontiers are (43,844.74, 3,507,770,000) for both MMOPSO and NSGA-II, with X and Y again representing the objective functions. Consequently, considering these Pareto frontier values, the proposed algorithm demonstrates its applicability and effectiveness in addressing the large-scale problem presented by this case study. Fig. 11 displays a comparison of the CPU times. It is evident that the CPU time for the epsilon-constraint method exhibits an exponential increase as the problem dimensions grow. In contrast, the CPU times for both NSGA-II and MMOPSO approaches are considerably less than that of the epsilon-constraint method. Notably, as the problem scale expands, the rate at which the CPU time increases for MMOPSO is significantly lower than that observed for NSGA-II.

Table 16: Established distribution centers, their optimum capacity and quantity of stored inventory.

No.	Scale	Period 1			Period 2				
		Food	Water	Tent	No.	Scale	Food	Water	Tent
1	Large	200,196	112,453	35,417	1	Large	200,150	300,215	11,705
2	Large	183,041	120,100	25,710	2	Medium	110,412	115,210	26,547
3	Medium	121,050	85,210	22,280	3	Medium	98,234	129,111	29,218
4	Small	14,411	15,211	9523	4	Small	16,210	22,140	4218
5	Large	225,400	285,547	29,218	5	Large	215,580	301,785	10,810
6	Medium	130,400	102,110	21,410	6	Small	15,410	20,142	5800
7	Large	241,180	152,450	29,550	7	Large	200,410	184,465	110,550
8	Small	11,508	21,580	5544	8	Small	9100	22,120	6517
9	Large	250,322	100,250	30,025	9	Large	200,173	200,300	71,258



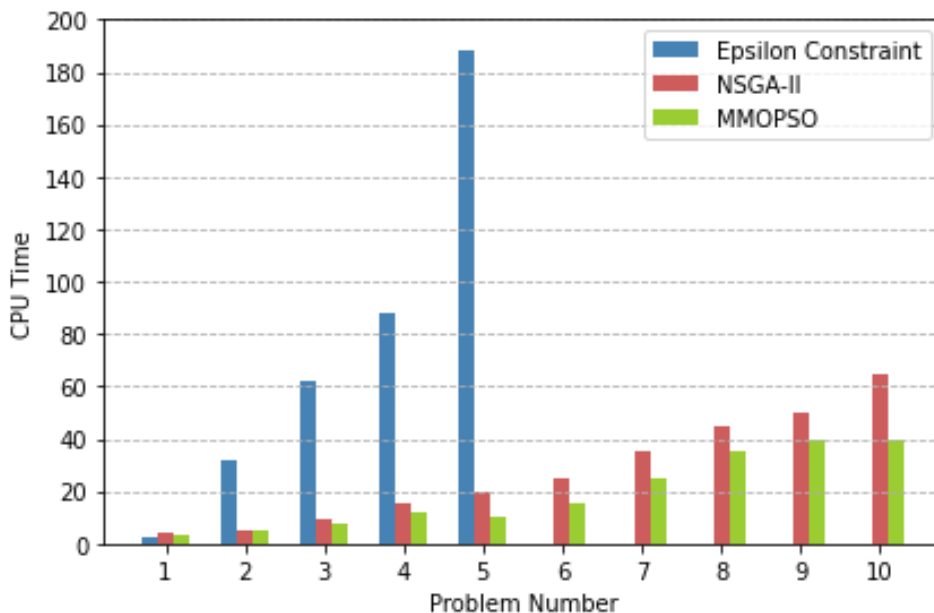


Table 17: Established accommodation centers and quantity of stored inventory.

Period 1				Period 2			
No.	Food	Water	Tent	No.	Food	Water	Tent
1	180,250	280,145	12,150	1	153,250	210,756	65,361
2	200,550	286,980	13,850	2	153,450	190,950	65,941
3	223,367	280,256	26,720	3	155,750	225,900	68,257
4	165,500	200,100	27,944	4	161,700	200,010	69,017
5	180,200	200,140	14,500	5	140,402	190,570	59,180
6	180,210	205,410	30,562	6	140,602	215,010	70,882
7	180,215	208,204	71,918	7	162,085	190,810	71,950

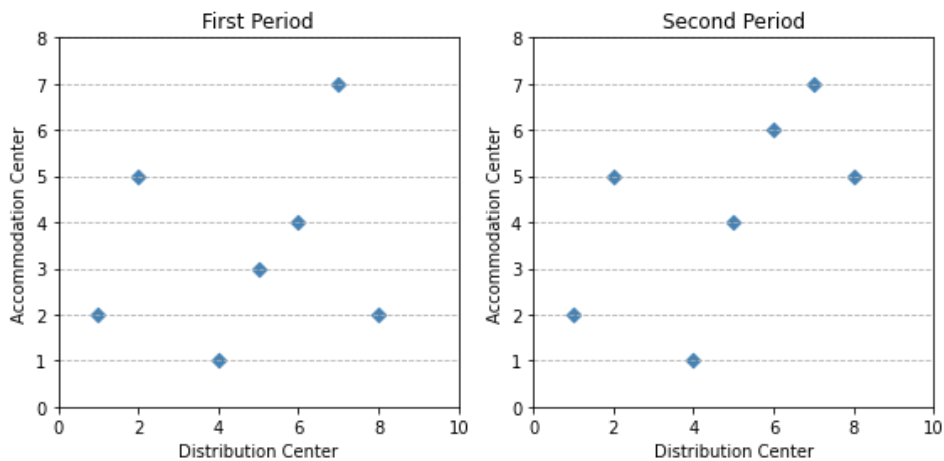


Figure 12: Allocation of accommodation centers to distribution centers

5.8 Mechanism of selecting preferred solution from non-dominated solutions

The Pareto frontier is comprised of a set of non-dominated solutions, each possessing its own unique structure and decision variables. Therefore, a method is necessary to select the most suitable preferred solution from this collection of non-dominated options. According to expert opinions, the importance of the second objective function is deemed to be twice that of the first objective function. This prioritization ensures that the minimization of shortage is given precedence over the cost of disaster relief operations. Consequently, the solution that exhibits the least amount of shortage is designated as the preferred solution. The preferred solution choice among the non-dominated set is Pareto solution No. 8. Since the MMOPSO algorithm yielded superior solutions, Pareto solution No. 8 generated by MMOPSO is chosen to exemplify the decision variables within a scenario (key fault in the night). Table 16 illustrates the decision variables associated with Pareto solution No. 8. It should be noted that Table 16 accounts for 9 distribution centers. Table 17 presents the established accommodation centers and the quantity of stored inventory for both the first and second periods specifically for Pareto solution No. 8. It is confirmed that, according to Table 17, 7 accommodation centers were established during each period. Fig. 12 visually represents the allocation of accommodation centers to various distribution centers for Pareto Solution No. 8. For instance, in the initial period, accommodation centers 2, 5, and 3 are assigned to distribution centers 1, 2, and 3, respectively. Similarly, in the second period, accommodation centers 2, 5, and 4 are allocated to distribution centers 1, 2, and 3, respectively.

CONCLUSION

This study developed an uncertain multi-objective, multi-commodity, multi-period, and multi-vehicle location-allocation mixed-integer programming model tailored for the rapid response phase following a disaster due to global warming impact. The proposed model encompasses five distinct echelons: affected communities, primary distribution hubs, medical facilities (hospitals), temporary shelter establishments, and temporary care facilities. To address the inherent uncertainties within the model, a probabilistic scenario-based methodology was adopted. The optimization strategy focused on two primary objectives: minimizing the overall cost associated with facility location and allocation, and concurrently minimizing the unmet demand for vital relief supplies. Significant decisions derived from the model include the strategic placement of temporary care and accommodation centers, the assignment of affected populations to established centers and hospitals, the allocation of distribution centers to temporary shelters, the optimized flow of both injured individuals and essential commodities across all facilities, the determination of optimal vehicle numbers for inter-facility transport, and the management of shortage and inventory levels at each center. The model incorporates a comprehensive set of constraints applied across multiple planning periods to ensure practicality and effectiveness. The developed model was rigorously evaluated using three distinct solution approaches: the epsilon-constraint method, NSGA-II, and MMOPSO. Initially, the performance of these algorithms was assessed through a series of random test instances of varying scales. A thorough statistical analysis, complemented by multi-objective performance evaluation metrics, was conducted to identify the most effective solution approach, ultimately confirming MMOPSO as the superior method. Subsequently, the validated model was applied to a real-world case study centered on the city of Warri and its environs, a region acutely susceptible to flooding exacerbated by the effects of global warming. The superior MMOPSO algorithm was then exclusively utilized to solve and analyze this specific case study.

In line with the study's commitment to social equity, the model inherently prioritizes the most vulnerable populations by aiming to minimize shortages of relief supplies. From the set of non-dominated solutions generated by MMOPSO for the Warri case study, a preferred solution was carefully chosen based on expert opinion, emphasizing the critical objective functions relevant

to equitable disaster response. The structural details and associated decision variables of this preferred solution were then thoroughly examined and discussed in the context of the specific challenges faced by Warri. Furthermore, a comprehensive sensitivity analysis was performed on crucial model parameters that are prone to variation in real-life disaster scenarios, including the probability of flood occurrence and the potential failure rates of humanitarian centers. The insights gained from this sensitivity analysis were meticulously scrutinized. Results indicated that an increase in the number of affected individuals necessitates an expansion in the establishment of accommodation centers. Moreover, a heightened probability of failure for temporary care and accommodation centers directly correlates with an increase in overall relief costs.

For future research, several promising avenues are suggested. Incorporating the explicit routing of relief distribution vehicles and the evacuation of affected individuals into the problem formulation would offer valuable enhancements. Additionally, exploring alternative methodologies for modeling parameter uncertainty, such as fuzzy sets or robust optimization approaches, could further refine the model's adaptability to unpredictable disaster environments.

REFERENCES

1. Ahmadi, M., Seifi, A., and Tootooni, B. (2015). Humanitarian logistics model for disaster relief operation considering network failure and resource limitation. *Transportation Research Part E: Logistics and Transportation Review*, 75, 145–163. <https://doi.org/10.1016/j.tre.2014.12.007>
2. Akbari, S. and Salman, F. S. (2017). Multi-objective robust optimization for emergency resource allocation. *Computers & Operations Research*, 88, 151–163. <https://doi.org/10.1016/j.cor.2017.07.014>
3. Barbarosoglu, G. and Arda, Y. (2004). A two-stage stochastic programming framework for transportation planning in disaster response. *Journal of the Operational Research Society*, 55(1), 43–53. <https://doi.org/10.1057/palgrave.jors.2601627>
4. Chen, J., Zhang, Y., Liu, W., and Huang, Y. (2022). An equity-integrated model for shelter resource allocation in disaster response. *Annals of Operations Research*. <https://doi.org/10.1007/s10479-021-04220-w>
5. Daneshvar, M. and Khadem, M. (2022). A robust multi-period optimization model for humanitarian relief supply under climate change uncertainty. *Sustainable Operations and Computers*, 3, 112–122. <https://doi.org/10.1016/j.susoc.2022.03.004>
6. Djalante, R., Shaw, R., and DeWit, A. (2020). Building resilience against biological hazards and pandemics: COVID- 19 and its implications for the Sendai Framework. *Progress in Disaster Science*, 6, 100080. <https://doi.org/10.1016/j.pdisas.2020.100080>
7. Farahani, R. Z., Rezapour, S., Drezner, Z., and Fallah, S. (2009). Competitive supply chain network design: An overview of classifications, models, solution techniques and applications. *Omega*, 45, 92–118. <https://doi.org/10.1016/j.omega.2013.08.006>
8. Ghasemi, P. and Khalilzadeh, M. (2019). A chance-constrained programming approach to humanitarian logistics under uncertainty. *Journal of Humanitarian Logistics and Supply Chain Management*, 9(1), 108–127. <https://doi.org/10.1108/JHLSCM-04-2018-0023>
9. Jabbarzadeh, A., Fahimnia, B., and Sabouhi, F. (2016). Resilient and sustainable supply chain design: Sustainability analysis under disruption risks. *International Journal of Production Research*, 56(1–2), 594–615. <https://doi.org/10.1080/00207543.2017.1370149>.

10. Kellermann, A. L., Savić, M., and Jones, M. (2018). Equity in disaster response: A critical perspective on distributional fairness in emergency logistics. *Disasters*, 42(S1), S99–S121. <https://doi.org/10.1111/disa.12226>
11. Li, H., Wang, Y., and Wu, J. (2022). Equity-oriented humanitarian logistics model incorporating social vulnerability data. *Computers & Industrial Engineering*, 171, 108432. <https://doi.org/10.1016/j.cie.2022.108432>
12. Liu, Y., Ma, J., Zhang, Z., and Gao, H. (2023). Hybrid evolutionary optimization for equitable disaster relief logistics. *Applied Soft Computing*, 129, 109658. <https://doi.org/10.1016/j.asoc.2022.109658>
13. Mohammadi, M., Ghazanfari, M., and Alinaghian, M. (2022). A robust optimization approach for resource allocation in humanitarian logistics considering social vulnerability. *Annals of Operations Research*. <https://doi.org/10.1007/s10479-022-04817-1>
14. Moradi, M. and Manzouri, M. (2024). Resilient food distribution network design during climate-induced crises. *Sustainable Production and Consumption*, 41, 201–213. <https://doi.org/10.1016/j.spc.2024.03.006>
15. Mohammed, M., Conchoa, A. L., and Ramirez Marquez, J. E. (2019). Evolutionary optimization framework for emergency resource allocation under uncertainty. *Reliability Engineering & System Safety*, 188, 1–10. <https://doi.org/10.1016/j.ress.2019.03.031>
16. Rahmani, D. and Ghasemi, P. (2022). Integrated location-inventory-routing optimization for climate-induced disaster logistics. *Computers & Industrial Engineering*, 169, 108233. <https://doi.org/10.1016/j.cie.2022.108233>
17. Ransikarbum, K. and Mason, S. J. (2016). Goal programming-based post-disaster humanitarian needs assessment under uncertainty. *Transportation Research Part E: Logistics and Transportation Review*, 95, 1–27. <https://doi.org/10.1016/j.tre.2016.08.007>
18. Rawls, C. G. and Turnquist, M. A. (2010). Pre-positioning of emergency supplies for disaster response. *Transportation Research Part B: Methodological*, 44(4), 521–534. <https://doi.org/10.1016/j.trb.2009.08.003>
19. Rawls, C. G. and Turnquist, M. A. (2016). Stochastic optimization for pre-disaster planning of emergency supply chains. *Journal of Infrastructure Systems*, 22(1), 04015016. [https://doi.org/10.1061/\(ASCE\)IS.1943-555X.0000279](https://doi.org/10.1061/(ASCE)IS.1943-555X.0000279)
20. Tofighi, S., Torabi, S. A., and Mansouri, S. A. (2016). Humanitarian logistics network design under mixed uncertainty. *European Journal of Operational Research*, 250(1), 239–250. <https://doi.org/10.1016/j.ejor.2015.09.045>
21. Torabi, S. A., Tofighi, S., and Heydari, J. (2018). Integrated evacuation planning and relief distribution under supply chain disruption and uncertainty. *Transportation Research Part E: Logistics and Transportation Review*, 115, 87–112. <https://doi.org/10.1016/j.tre.2018.05.001>
22. Tzeng, G.-H., Cheng, H.-J., and Huang, T. D. (2007). Multi-objective optimal planning for designing relief delivery systems. *Transportation Research Part E: Logistics and Transportation Review*, 43(6), 673–686. <https://doi.org/10.1016/j.tre.2006.10.012>
23. Wang, Y., Li, H., and Zhou, Y. (2021). Renewable energy-powered UAV applications in emergency logistics under resource constraints. *Sustainable Cities and Society*, 75, 103328. <https://doi.org/10.1016/j.scs.2021.103328>
24. Wu, Y. and Cui, N. (2021). A bi-objective flood evacuation planning model integrating climate projections. *Natural Hazards*, 108(1), 1001–1027. <https://doi.org/10.1007/s11069-021-04856-3>

25. Yazdani, M., Zavadskas, E. K., and Chatterjee, P. (2021). Dynamic network reconfiguration in flood-affected logistics systems. *Journal of Cleaner Production*, 283, 124597. <https://doi.org/10.1016/j.jclepro.2020.124597>
26. Yuan, Z., Gao, L., Zhang, X., and Liu, Y. (2023). Equity in humanitarian logistics: A Gini-based optimization approach. *Operations Research for Health Care*, 39, 100387. <https://doi.org/10.1016/j.orhc.2023.100387>
27. Zheng, Y., Gao, L., and Zhang, H. (2019). Multi-commodity flow-based disaster relief logistics optimization under uncertainty. *Computers & Industrial Engineering*, 127, 765–778. <https://doi.org/10.1016/j.cie.2018.11.042>
28. Zhu, X., Li, J., and Qian, X. (2020). Max-min fairness optimization for emergency shelter location allocation. *Transportation Research Part E: Logistics and Transportation Review*, 140, 101961. <https://doi.org/10.1016/j.tre.2020.101961>